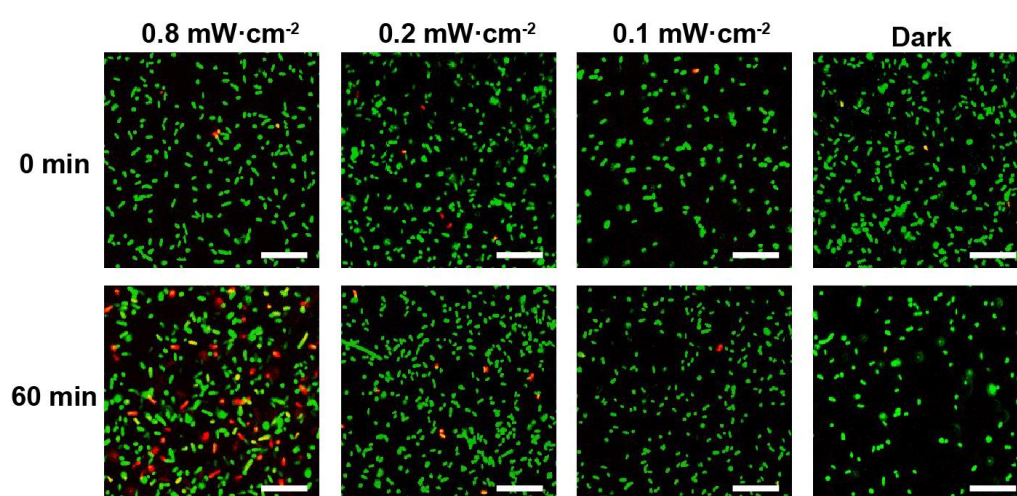


## Supporting Information

# Synthetic Cells with Chemo–Optical Signaling Enable Targeted Capture and Killing of Bacteria

*Xiaoran Zheng, Tarek S. Elsayed, Yanjun Zheng, Matthew E. Allen, Seraphine V.*

*Wegner\**



**Figure S1. Phototoxicity analysis of bacteria under varying light intensities.** Confocal microscopy images of bacteria stained with a LIVE/DEAD bacterial viability kit (green: total bacteria; red: dead bacteria) at 0 and 60 min under continuous blue-light illumination at different intensities and in the dark. While pronounced phototoxicity is observed at 0.8 mW·cm<sup>-2</sup> after 60 min, lower intensities (0.2 mW·cm<sup>-2</sup> and 0.1 mW·cm<sup>-2</sup>) show negligible effects on bacterial viability, comparable to the dark control. Scale bars are 50 μm.

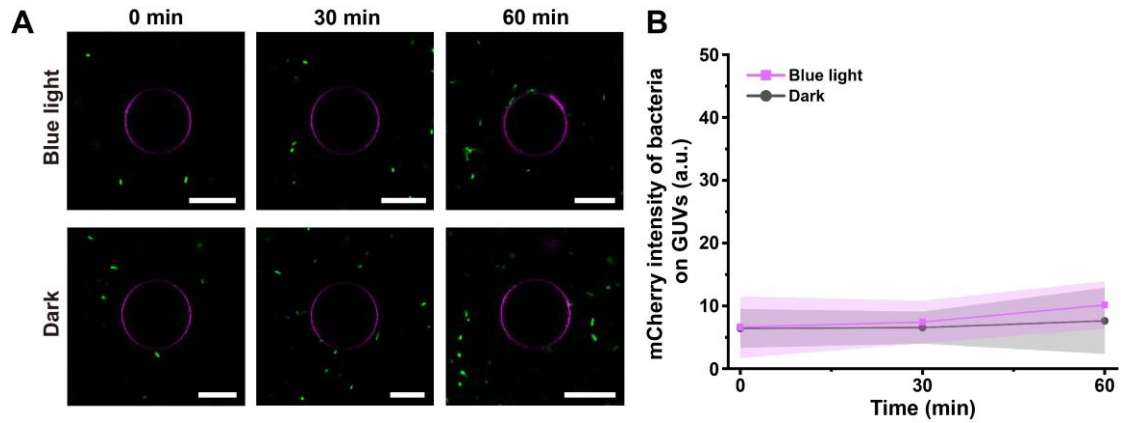


**Figure S2. Minimal bacterial interactions with non-functionalized GUVs.** (A) Representative confocal microscopy images showing background level interactions between bacteria (green) and GUVs lacking BcLOV4-mCherry functionalization (magenta) under blue light illumination and in the dark. Scale bars are 20  $\mu\text{m}$ . (B) Time course of bacterial fluorescence intensity at the GUV surface. Data are presented as the mean of three independent experiments (total  $n \geq 25$  GUVs).

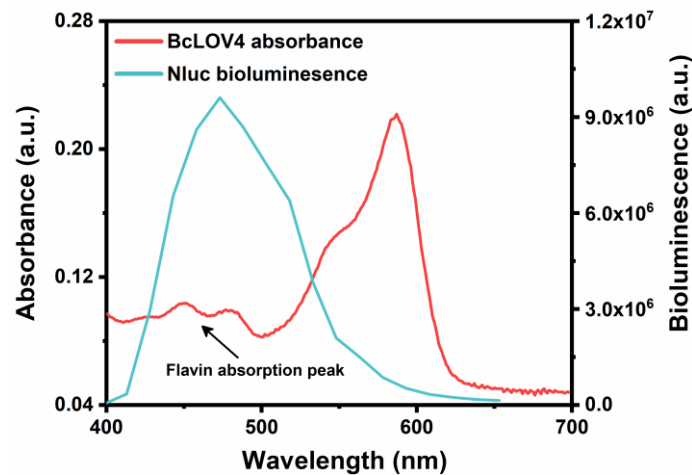


**Figure S3.** Absorption spectrum of BcLOV4-mCherry and bioluminescence emission spectrum of Nluc. The flavin absorption of BcLOV4 around 450 nm coincides with the emission maximum of the Nluc luminescence.

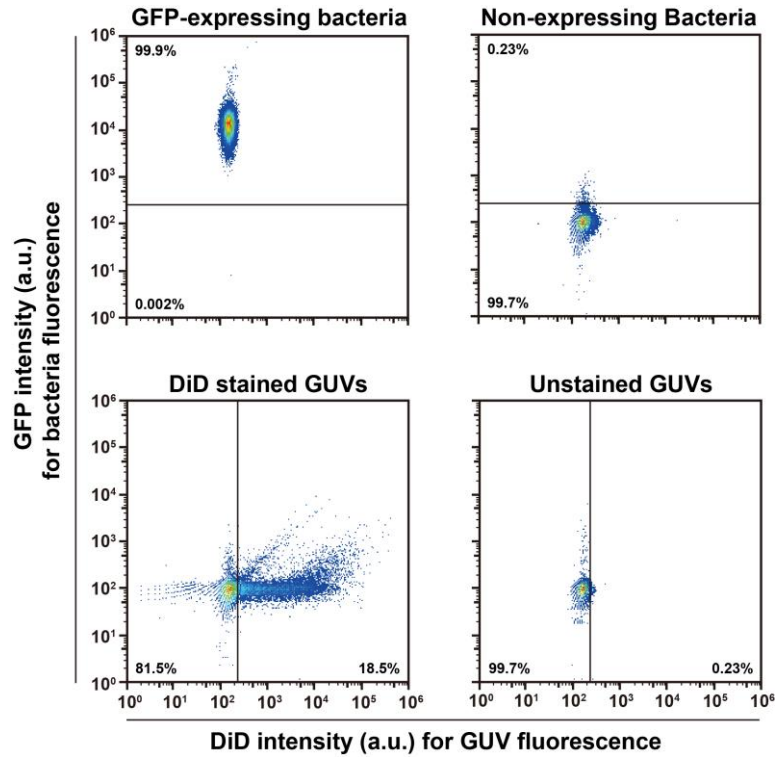


**Figure S4. Gating strategy for flow cytometry analysis.** Dual-channel scatter plots (DiD vs. GFP) of control samples used to define the quadrant gating strategy used in Figure 3F. Upper panels: comparison of GFP-expressing bacteria with non-expressing bacteria to set the threshold in the GFP channel. Lower panels: comparison of DiD-stained GUVs with unstained GUVs to distinguish GUV associated signals in the DiD channel. Horizontal and vertical thresholds were set at the 99.7% boundary of the respective negative control populations, ensuring exclusion of background events.

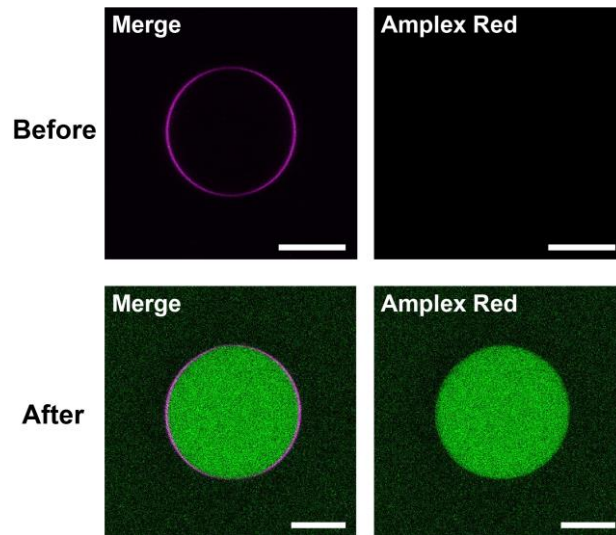


**Figure S5. Validation of GaoA activity on GUVs.** Confocal microscopy images of a GaoA-BcGUV (magenta) before and after the addition of the reaction mixture (0.1  $\mu\text{M}$  HRP, 1 mM galactose, and 50  $\mu\text{M}$  Amplex Red). Scale bars are 10  $\mu\text{m}$ . Following addition of the reaction mixture, a strong fluorescence resorufin signal (green) is observed primarily within the GUV, confirming the successful generation of  $\text{H}_2\text{O}_2$  to initiate the signaling cascade.

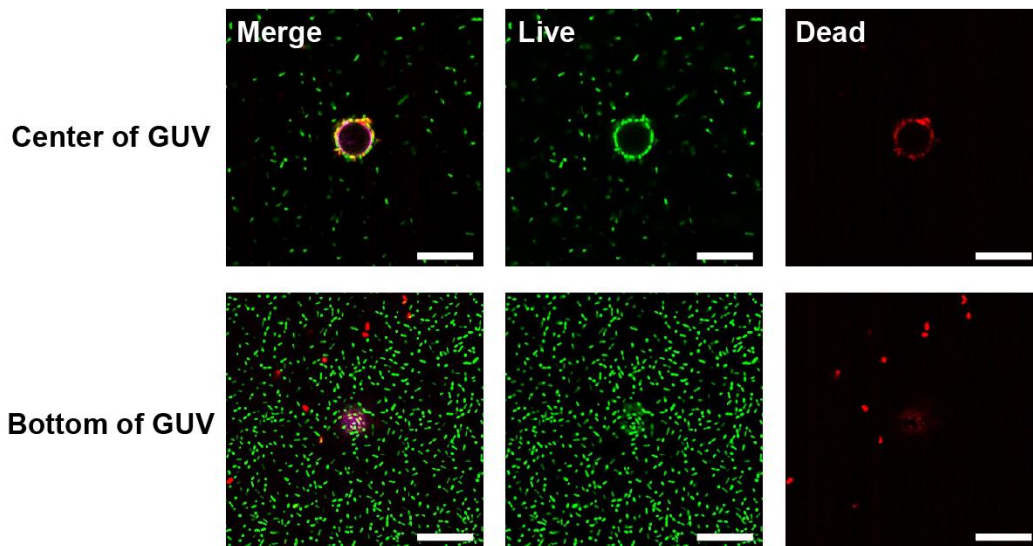


**Figure S6. Spatially confined bacterial elimination.** Confocal fluorescence images showing colocalization of the dead bacterial cell signal only at the GUV surface (magenta), indicating the selective killing of captured bacteria (red) while distal bacteria at the bottom of the GUV remain viable (green). Scale bars are 10  $\mu\text{m}$ .

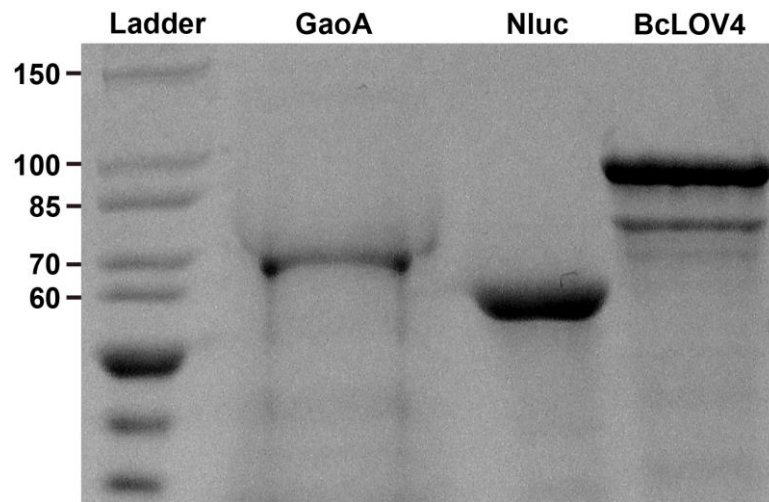


**Figure S7. SDS-PAGE analysis of purified proteins.** Lane 1: Molecular weight ladder. Lane 2: GaoA (72 kDa). Lane 3: Nluc (61 kDa). Lane 4: BcLOV4-mCherry (95 kDa).